



Article

Exposing Sustainable Mortars with Nanosilica, Zinc Stearate, and Ethyl Silicate Coating to Sulfuric Acid Attack

Victoria Eugenia García-Vera ¹, Antonio José Tenza-Abril ^{2,*}, Marcos Lanzón ¹ and José Miguel Saval ²

¹ Departamento de Arquitectura y Tecnología de la Edificación, Universidad Politécnica de Cartagena, 30203 Murcia, Spain; victoria.eugenia@upct.es (V.E.G.-V.); marcos.lanzon@upct.es (M.L.)

² Department of Civil Engineering, University of Alicante, 03690 Alicante, Spain; jm.savall@ua.es

* Correspondence: ajt.abril@ua.es; Tel.: +34-96-5903-400 (ext. 2729)

Received: 17 September 2018; Accepted: 16 October 2018; Published: 18 October 2018



Abstract: Obtaining durable materials that lengthen the service life of constructions and thereby contribute to sustainability requires research into products that improve the durability of cementitious materials under aggressive conditions. This paper studies the effects of sulfuric acid exposure on four mortar types (control mortar, mortar with nanosilica, mortar with zinc stearate, and mortar with an ethyl silicate coating), and evaluates which of them have better performance against the acid attack. After 28 days of curing, the samples were exposed to a sulfuric acid attack by immersing them in a 3% *w/w* of H₂SO₄ solution. Physical changes (mass loss, ultrasonic pulse velocity, open porosity, and water absorption), and mechanical changes (compressive strength) were determined after the sulfuric acid exposure. A scanning electron microscope (SEM) was used to characterize the morphology of the surface mortars after the exposure. The control mortar had the highest compressive strength after the acid attack, although of the four types, the zinc stearate mortar showed the lowest percentage of strength loss. The zinc stearate mortar had the lowest mass loss after the acid exposure; moreover, it had the lowest capillary water absorption coefficient (demonstrating its hydrophobic effect) both in a non-aggressive environment and acid attack.

Keywords: zinc stearate; nanosilica; ethyl silicate; sulfate exposure; sulfuric acid attack; durability

1. Introduction

Nature and the environment are not an inexhaustible source of resources, and their protection and rational use are necessary. Therefore, it is vital to work with durable materials that extend the service life of constructions. This contributes to the saving of existing resources and avoids causing harm to the environment. It is especially difficult to stretch the service life of cement-based materials when they are exposed to aggressive chemical environments. This is the case of some infrastructures that are affected by chemical attacks, such as sanitation networks, foundations [1,2], and infrastructures in contact with groundwater or in agricultural and farm facilities. These types of attacks are one of the most severe mechanisms in the deterioration of cementitious materials, so it is important to research products that contribute to prolonging the durability of these materials. This is one of the reasons why the use of admixtures and additives in cement-based materials has become very popular [1,3–5].

External sulfate exposures have a detrimental impact on cementitious materials [6,7], such as concretes and mortars. An externally-sourced sulfate attack is a slow process that can take years to manifest itself, causing internal changes in the microstructure. These changes are manifested in physical and mechanical alterations such as strength loss, mass variation, cracking, softening,

decohesion, etc. [8,9]. There are two types of sulfate attacks, which can be classified as either chemical or physical. Chemical attacks are common in buried concretes exposed to acidic sulfate waters existing in groundwater, where the sulfates react with aluminates hydrates to produce ettringite and gypsum. When a concrete is submerged in sulfate water, a physical attack can occur due to the crystallization of sulfate salts inside the pores of the concrete when it dries. This attack mechanism is usual in tidal zones where there are cycles of wetting and drying [10].

The chemical corrosion by sulfuric acid is not a pure sulfate attack, but an attack by free sulfuric acid is more severe than any with a neutral sulfate solution. Sulfuric acid may be present in ground waters, some industrial waste-waters, in sewers, and in rain water coming from industrial areas. In this type of attack, the sulfuric acid reacts with the by-products of cement hydration producing gypsum and amorphous hydrous silica in the reaction with the calcium silicate hydrate phase (C-S-H), gypsum in the reaction with the calcium hydroxide, and gypsum and aluminum sulfate in the reaction with the calcium sulfoaluminate hydrate phases. The chemical reactions that take place produce a profound degradation of the hydrated cement paste, and is associated with a loss of strength [11,12]. This study is focused on the effects of a sulfuric acid attack on cement mortars.

To obtain durable mortars and concretes that can withstand sulfuric acid attacks, the following procedures are necessary among others: (i) controlling the materials used during the manufacturing process, (ii) manufacturing with a low water/cement ratio [13–15], and (iii) guaranteeing suitable curing conditions [8,16]. Moreover, it is possible to use admixtures or additives to extend the durability of cement-based materials. Nanomaterials in concrete and cement mixtures are used to enhance its performance and durability [17–19]. Nanotechnology is not only able to increase the compressive and flexural strength, but it also reduces the porosity and water absorption of the cement mixtures [17,20]. Examples of nanomaterials used in cement-based materials are nanosilica [21], nanoalumina [22], titanium oxide [23], carbon nanotubes [24], and polycarboxylates [25]. Mortars containing nanosilica reduce the loss of both mass and compressive strength after an acid attack. This is because the nanosilica refines the pore structure, creating a more compact microstructure, which reduces porosity and absorptivity [26].

Water-repellent admixtures can also contribute to increasing the durability of the cement-based materials since water absorption represents one of the most important degradation factors for porous construction materials (e.g., mortars, stones, bricks, and concretes) [27]. There are diverse hydrophobic compounds that can be used as admixtures and provide waterproofing properties to mortars such as powdered stearates, oleates, and products based on silanes and silicones [28,29]. Moreover, water-repellent admixtures can help to enhance the resistance of the cementitious materials to acid environments because they reduce the affinity of capillary pore surfaces to moisture [30]. Zinc stearate is one of the most frequently used materials to achieve hydrophobic mixtures [31]. It is used with different types of binders, such as cements, clays, and limes, and its effectiveness in aggressive environments was proven even on adobe materials exposed to an acid-rain attack [32]. Ethyl silicate is a liquid solution that is applied in the form of a coating and its use has been widely utilized for stone consolidation. The ethyl silicate reacts with the substrate on which it is applied, and after curing, has a pozzolanic effect. However, although ethyl silicate is not a water-repellent additive, it decreases the capillary suction of the cement-based materials [33]. Nevertheless, this material, like zinc stearate, has not been extensively studied on cementitious materials exposed to chemical attacks.

Studying the behavior of mortars with different additions, especially against sulfuric acid attack that contain zinc stearate and ethyl silicate, is a topic needing more investigation because the studies in this field are limited. The aim of this study is to investigate the effect on the physical and mechanical properties of four different types of mortars after exposure to a sulfuric acid attack: (i) a control mortar without additions, (ii) a mortar with nanosilica, (iii) a mortar with zinc stearate, and (iv) a mortar with an ethyl silicate coating.

2. Materials and Methods

2.1. Materials

Four types of mortars were studied: (i) control mortar (C Mortar), (ii) mortar with nanosilica (NS Mortar), (iii) mortar with zinc stearate (ZS Mortar), and (iv) mortar with an ethyl silicate coating (ES Mortar).

Limestone fine aggregate sand was used. Figure 1 shows the particle-size distribution of the limestone fine aggregate carried out according to the EN 933-1 standard [34]. The limestone fine aggregate to binder ratio was 3:1 as prescribed by standard EN 196-1 [35], and the water to binder ratio was 0.45. To maintain the workability of all four mortars, superplasticizer (Sika ViscoCrete-5980, Sika SAU, Madrid, Spain) amounting to 1.5% of the cement weight was added. The NS mortar was manufactured by adding amorphous nanosilica suspension (BASF MasterRoc MS 685, BASF Construction Chemicals España, S.L. Barcelona, Spain), amounting to 2% of the cement weight. The ZS mortar was manufactured by adding zinc stearate (Alfa Aesar, Ward Hill, MA, USA), amounting to 2% of the cement weight. The ES mortar was carefully spray-coated with ethyl silicate (Silikat Tes 40 WN, Wacker Chemie AG, Munich, Germany).

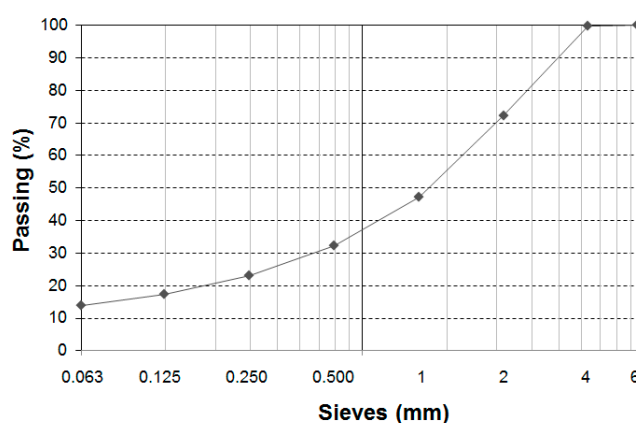


Figure 1. Particle-size distribution of the limestone fine aggregate.

Chemical–Physical Characterization of the Binder

An ordinary Portland cement CEM I 52.5 R (CEMEX, Madrid, Spain) according to the standard EN 197-1 [36], was used to produce the mortars. The crystallographic phases were identified in the cement by using X-ray diffraction (XRD) carried out with a Bruker D8-Advance diffractometer (Bruker Española S.A., Madrid, Spain). The X-ray tube was operated at 40 kV and 40 mA, and the spectra were registered with angles from 4° to 60° at 0.05° stepping intervals in Θ - Θ mode. In addition, the chemical composition of the cement was obtained using X-ray fluorescence (XRF) with an X-ray sequential spectrometer PHILIPS MAGIC PRO (Philips Ibérica, Madrid, Spain). The XRD analysis in Figure 2 shows the following major phases in Portland cement: (C_3S), (C_2S), (C_4AF) and calcite. The XRF results (Table 1) show the binder was mainly composed of CaO and SiO_2 as expected for calcium silicates (C_3S and C_2S). The percentage of SO_3 can be explained by the addition of gypsum (as shows the XRD in Figure 2), which is the set retarder for ordinary Portland cement.

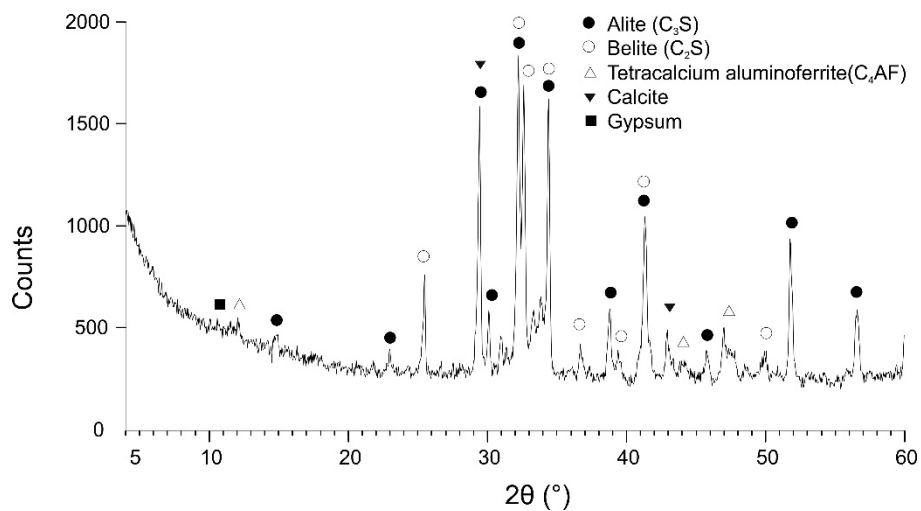


Figure 2. X-ray diffraction spectrum of the Portland Cement CEM I 52.5 R.

Table 1. XRF characterization of CEM I 52.5 R.

	Percentage (%)
Na ₂ O	0.23
MgO	3.29
Al ₂ O ₃	3.36
SiO ₂	14.89
P ₂ O ₅	0.14
SO ₃	4.62
Cl	0.11
K ₂ O	1.06
CaO	55.36
TiO ₂	0.25
MnO	0.04
Fe ₂ O ₃	3.06
SrO	0.12
Other elements	<0.30

2.2. Methods

2.2.1. Manufacturing and Curing Process of the Mortars and Sulfuric Acid Attack Simulation

The tests were carried out on prismatic specimens with standardized dimensions (40 × 40 × 160 mm) that were manufactured according to the standard EN 196-1 [35]. A total of 24 specimens were manufactured, 6 per each type of mortar. After the first 24 h, the specimens were de-molded and were kept in a humidity chamber for 28 days at 95 ± 2% of relative humidity and 20 ± 2 °C. The specimens that had to be coated with ethyl silicate (ES mortars) were taken out from the humidity chamber in the midst of the curing process only for the time necessary to carry out the spray coating. The specimens were carefully spray-coated with ethyl silicate at a controlled distance of 10 cm, using a small airbrush (Figure 3d). After completing the coating, the specimens were returned to the humidity chamber to continue the curing process. After 28 days of curing, twelve specimens were exposed to a sulfuric acid attack simulation (three specimens per each type of mortar), and the other twelve were stored in standard laboratory conditions to use as reference samples.

The sulfuric acid attack was performed by immersing the specimens into a H₂SO₄ solution (3% w/w) (Figure 3a,b) in hermetically closed containers, this procedure has been used in previous studies [30]. A high concentration of sulfuric acid was chosen in order to accelerate their effects on the mortars, and obtain the same degradation in less exposition time [1]. The H₂SO₄ solution was changed

weekly to reduce the variation of the concentration of sulfuric acid. Finally, the containers were kept in a controlled-temperature room. The procedure for changing the solution was done as follows:

1. The specimens were extracted from the H_2SO_4 solution and were gently brushed under a weak flow of tap water to eliminate material residue that may have adhered to the surface.
2. The H_2SO_4 solution was replaced with a new solution.
3. The specimens were reintroduced into the new solution.

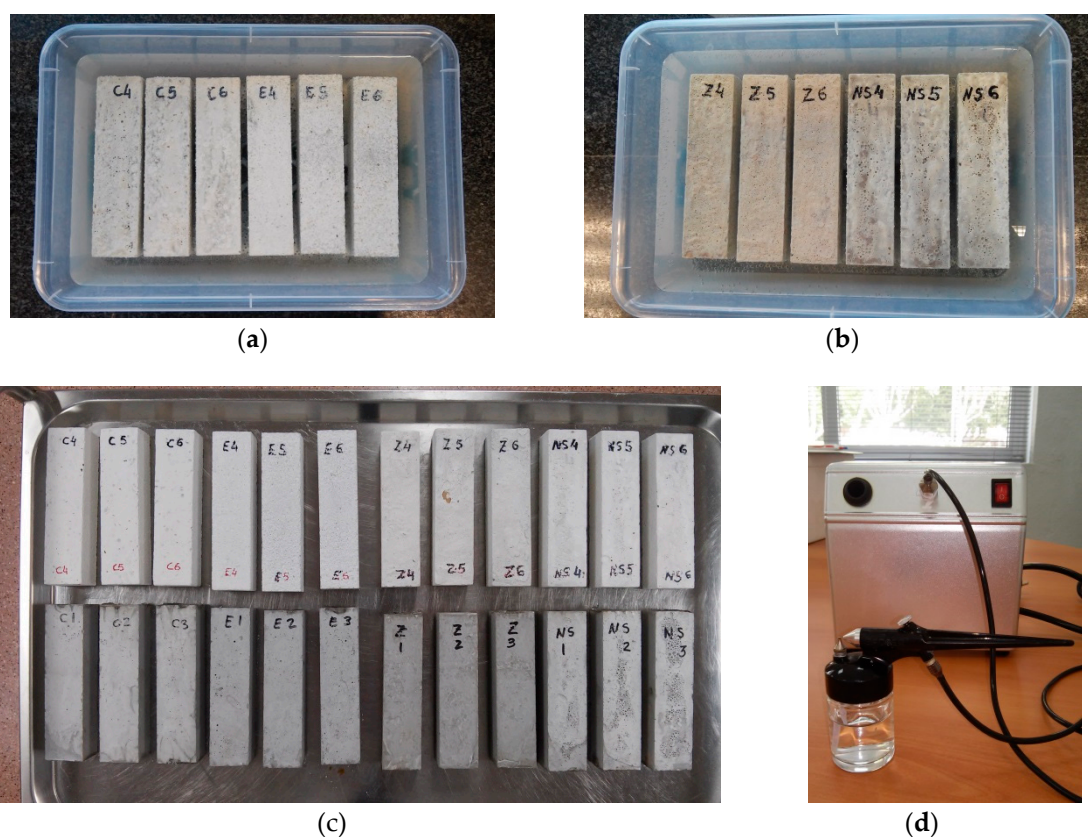


Figure 3. (a,b) Specimens immersed in the sulfuric acid solution (C = control mortar; E = mortar with an ethyl silicate coating; Z = zinc stearate mortar; NS = nanosilica mortar). (c) Specimens before testing at t_{56} . Upper row: specimens exposed to sulphuric acid; lower row: specimens with no acid attack. (d) Airbrush used to spray the specimens.

2.2.2. Physical and Mechanical Properties of the Mortars After the Sulfuric Acid Attack

The mass variation of the specimens exposed to the sulfuric acid was obtained by weighing the specimens six times during the acid attack period: (i) before starting the sulfuric acid exposure and hence at 28 days after their manufacture (t_{28}), (ii) at 7 days of acid exposure (t_{35}), (iii) at 14 days (t_{42}), (iv) at 21 days (t_{49}), (v) at 28 days (t_{56}), and (vi) at 90 days of acid exposure (t_{118}). The percentage of mass loss was calculated in relation to the initial weight, i.e., at t_{28} . The open porosity of the specimens exposed to the sulfuric acid attack was determined following the procedure of the standard EN 1936 [37], and it was calculated at 28 days (t_{56}) and 90 days (t_{118}) of acid exposure.

The ultrasonic pulse velocity test was performed following the EN 12504-4 standard [38]. The test consisted of measuring the propagation time of the ultrasonic waves along the longest dimension of the specimen (160 mm). Contact transducers emitting ultrasonic pulses at 54 kHz were coupled to the end sides of the specimens. Three determinations were made per sample. The test was performed for the specimens that had been exposed to the sulfuric acid attack and for those that had not been. The ultrasonic test was carried out at 28 days (t_{56}) of acid exposure, i.e., at 56 days from their manufacture.

The compressive strength tests were conducted according to the EN 196-1 standard [35] and were carried out at 28 (t_{56}) and 90 (t_{118}) days of sulfuric acid exposure (three samples per each exposition time and type of mortar).

The capillary water absorption coefficient was calculated for the reference samples (kept in standard laboratory conditions) and for the samples exposed to the sulfuric acid attack for 90 days (t_{118}), with the aim of comparing the difference of behavior. According to the standard EN 1015-18 [39], the coefficient was computed using the formula:

$$C = \frac{M_2 - M_1}{A(t_2^{0.5} - t_1^{0.5})}$$

where:

C = capillary water absorption coefficient, $\text{kg}/(\text{m}^2 \cdot \text{min}^{0.5})$

M_1 = specimen mass after the immersion for 10 min, kg

M_2 = specimen mass after the immersion for 90 min, kg

A = surface of the specimen face submerged in the water, m^2

t_2 = 90 min

t_1 = 10 min

2.2.3. Scanning Electron Microscopy (SEM) Examination

All the samples were examined with a scanning electron microscope Hitachi S3000N (Hitachi High-Technologies Canada, Inc., Toronto, Canada) in order to perform a microstructural analysis. The microscope was equipped with an X-ray detector Bruker XFlash 3001 (Bruker Española S.A., Madrid, Spain) for microanalysis EDX (energy-dispersive X-ray spectroscopy). To study the samples, small fragments were carefully removed from the surface and dried at 60 °C. For each sample, three EDX analyses were performed in three different zones, operating in variable pressure mode at 20 kV. The surface was studied in secondary electrons mode at an ultra-high vacuum using an accelerating voltage of 15 kV and the working distance was variable. Despite EDX being a semi-qualitative technique and it has some uncertainty, in this study it has been used to approximate the sample composition.

3. Results and Discussion

3.1. Compressive Strength

The progress of a sulfuric acid attack was evaluated by measuring the compressive strength. Figure 4 shows the compressive strength of the mortars tested under two curing conditions: non-aggressive environments, and aggressive environments with sulfuric acid attack. In the first case, non-aggressive environments, the strength of the mortars at t_{118} increased with respect the strength at t_{56} ; this increase is common in mortars that cure under standard conditions. The mortar with the ethyl silicate coating had the highest strength for t_{56} and t_{118} , and the zinc stearate mortar had the lowest strength, having lower strength at t_{56} than the control mortar, although at t_{118} , it was slightly higher. Figure 4c shows that for a non-aggressive environment, the control mortar maintained its strength; however, the other three mortars augmented their strength from t_{56} to t_{118} , possibly because the compressive strength increase of these mortars occurred over a long period.

In the second case, aggressive environments, the reduction in compressive strength was a direct effect of the sulfuric acid exposure due to the migration of sulfate ions into concrete accompanied by a gradual dissolution of Portlandite and decomposition of the C-S-H phase [40]. Simultaneously, the formation of more expansive compounds [41,42] and consequent volumetric strains in the hardened material were also considered to be responsible for expansive forces and micro-cracking [43]. As can be seen in Figure 4, the compressive strength for the mortars exposed to the sulfuric acid attack was lower than the compressive strength of the mortars that were not attacked, both at t_{56} and t_{118} . All the mortars presented strength loss in the time interval from t_{56} to t_{118} . The zinc

stearate mortar was the one with the lowest percentage compressive strength loss compared to the rest of mortars (Figure 4c). The percentage compressive strength loss observed in NS mortars are in line with those reported in the literature [13].

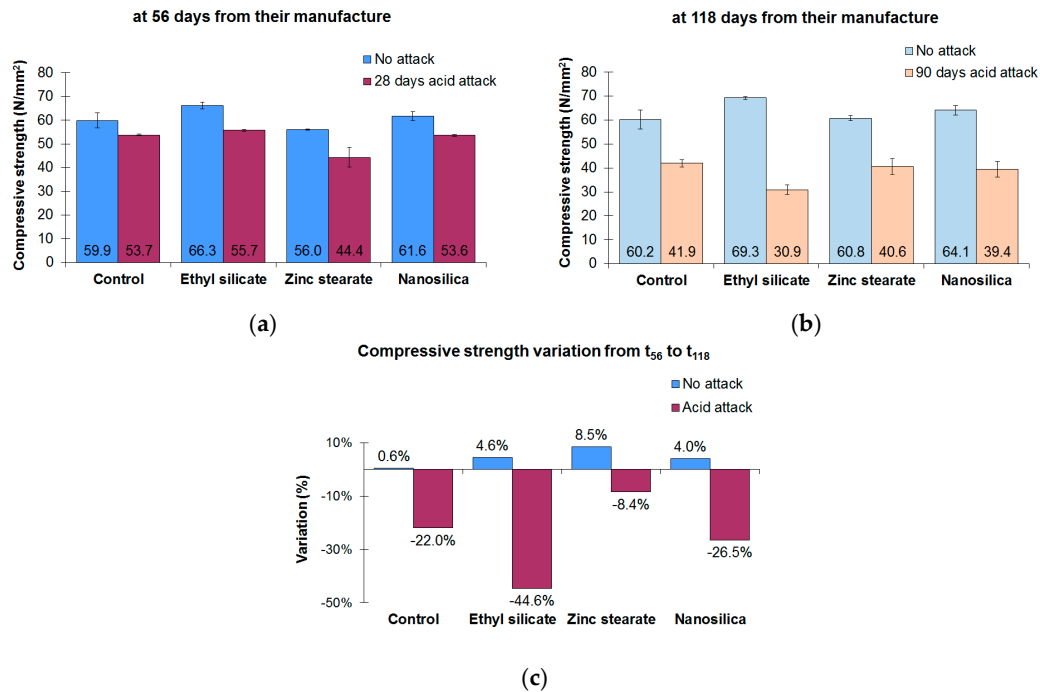


Figure 4. (a) Compressive strength at t_{56} (28 days of sulfuric acid attack), (b) compressive strength at t_{118} (90 days of sulfuric acid attack), and (c) variation percentage of the compressive strength from t_{56} to t_{118} for attacked and non-attacked mortars.

3.2. Mass Loss Due to the Sulfuric Acid Exposure

The analysis of the mass loss as a function of the exposure time to the sulfuric acid attack (Figure 5) showed that the resistance to the attack of the nanosilica mortar and the mortar treated with an ethyl silicate coating was similar to the control mortar. This result is consistent with other authors [8,13] who state that the sulfate resistance is generally higher at a lower water/cement ratio. However, the zinc stearate mortar was the one that best resisted the acid attack as its mass loss was lower than for the other mortars at t_{118} . The increment in mass loss and compressive strength loss observed when the exposure time increased are consistent with the results obtained in previous studies [26].

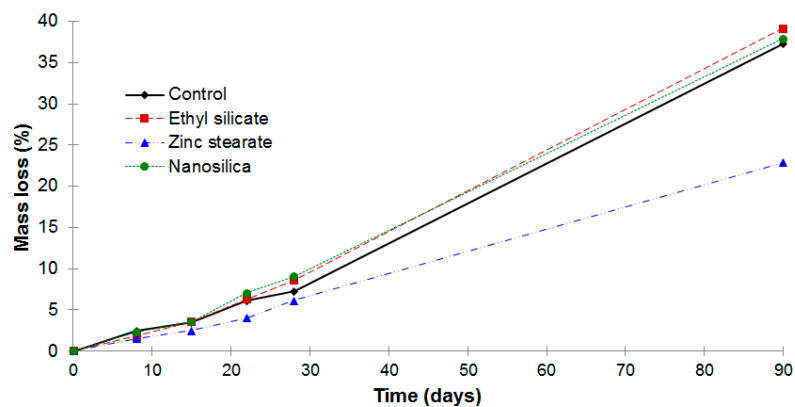


Figure 5. Mass loss as a function of the exposure time to the sulfuric acid attack.

The formation of ettringite and gypsum is common in cementitious systems exposed to sulfuric acid solutions and is observed in numerous field and laboratory studies [11,12,44]. Deleterious expansion occurs in mortars due to an excessive amount of these formations. The expansion is usually accompanied by the development of cracks in the mortar, initiated near the surface, and gradually evolving towards the central portion of the mortar [11]. As mentioned in Section 2.2.1, the specimens were brushed and cleaned weekly to remove the gypsum adhered to the specimen surface. As can be seen in Figure 5, the mass loss was mainly associated to the degradation of the mortar due to the formation of gypsum in the surface removed during the process.

3.3. Ultrasonic Pulse Velocity

Ultrasonic pulse velocity is based on a longitudinal wave pulse and it can be simply performed [45]. The ultrasonic propagation velocity obtained for all the mortars was similar except for the zinc stearate mortar that was the lowest. Some experimental studies have demonstrated that the measurement of the P-waves is suitable for estimating the changes in the dynamic modulus of concrete depending on the sulfate attack damage [46,47]. When the mortars were exposed to the sulfuric acid attack, a significant reduction of the ultrasonic pulse velocity was observed (Figure 6). The reduction reflects the deterioration caused by sulfuric acid attack, which provides information about the internal condition and quality of mortars [48–50].

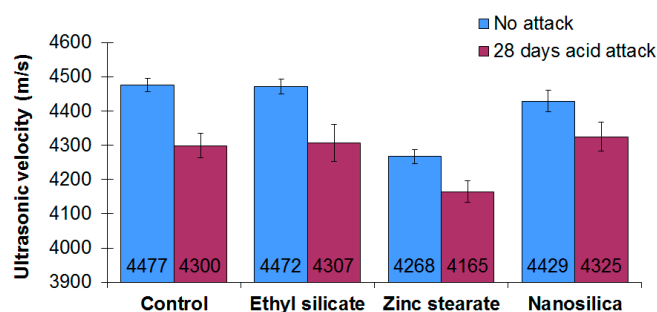


Figure 6. Ultrasonic velocity at t_{56} .

3.4. Open Porosity and Capillary Water Absorption Coefficient

Open porosity influences the durability of the cement-based materials because it affects the corrosion of reinforcing steel, which many authors consider to be the most grave pathology affecting reinforced concrete structures [1,51]. Figure 7 shows the open porosity evolution of the mortars attacked with the sulfuric solution from t_{56} to t_{118} . All the mortars presented a similar behavior, as they increased their open porosity in similar proportions from t_{56} to t_{118} , except for the ZS mortar, which had the highest increase in its open porosity. However, the open porosity percentage of the ZS mortar at t_{118} was the lowest open porosity compared with the other three mortars. The increment of the open porosity observed was related to the sulfate attack effects, which would involve the formation of expansive products [43], producing a loss of solid fraction in the mortar [2].

Figure 8 shows the capillary water absorption coefficients calculated according to the EN 1015-18 standard [39]. The coefficients were evaluated for the mortars at t_{118} , both the non-attacked mortars and the mortars attacked with the sulfuric solution. For the non-attacked mortars, the highest coefficient was obtained for the NS mortar, and as expected, the lowest coefficient was obtained for the ZS mortar. The capillary water absorption coefficients after 90 days of sulfuric acid exposure of the mortars reduced its value in similar proportions, except the ZS mortar that increased its coefficient to 82.0%. The reduction of the absorption coefficients for the mortars (C mortar, ES mortar, and NS mortar) may be due to the network of gypsum crystals that was compact enough to obstruct the capillary network [7] and can be seen in the SEM micrographs of the mortars attacked (Figure 9). It should be highlighted that the zinc stearate had a hydrophobic effect, and therefore, the ZS mortar

had the lowest absorption coefficient, both in a non-aggressive environment and under acid exposure. A possible reason for the increase of capillary water absorption found in ZS mortars is that the gypsum coating created on the surface was weaker and more external as compared to the C, ES, and NS mortars (Figure 9f). On the other hand, the observed differences were minimal considering the magnitude of the capillary water uptake.

Although the capillary water absorption coefficients were obtained according to the UNE EN 1015-18 standard (Figure 8), they were also obtained using linear regression for water absorption data as a function of time (Table 2). It was found that in almost all cases (except in the ZS mortar) the water absorption variation was practically linear, as shown by the values of the correlation coefficients (R^2) that are close to the unit. Moreover, the values of the regression line slopes obtained are almost the same as the obtained following the indications of the standard EN 1015-18 [39]. Therefore, as some authors show [52], the absorption coefficient can be obtained as the slope of the regression lines.

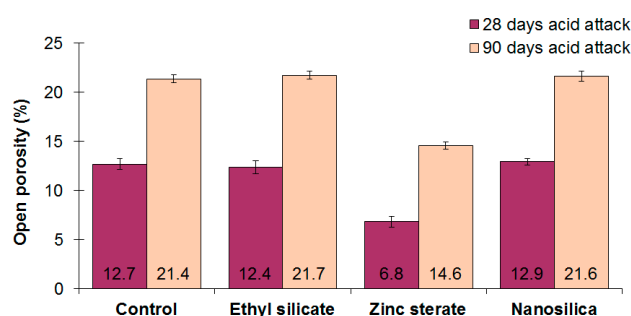


Figure 7. Open porosity after the sulfuric acid attack at t_{56} and t_{118} .

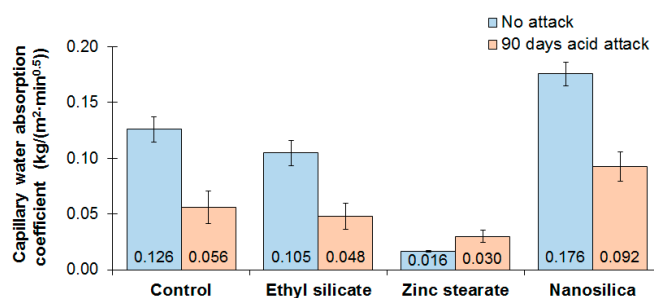


Figure 8. Capillary water absorption coefficient at t_{118} calculated according to the standard EN 1015-18 [39].

Table 2. Capillary water absorption coefficient at t_{118} calculated as the slope of the regression lines.

	No Attack		Sulfuric Acid Attack		Variation
	Regression Line Slope	R^2	Regression Line Slope	R^2	
Control	0.129	1.00	0.055	0.99	−57.6%
Ethyl silicate	0.105	1.00	0.045	0.97	−56.6%
Zinc stearate	0.015	0.98	0.029	0.94	89.2%
Nanosilica	0.175	1.00	0.090	0.99	−48.3%

3.5. Scanning Electron Microscopy (SEM) Examination

Degradation is usually found as a result of the severe external damage. The sulfuric acid attack created on the mortars' surface a layer of gypsum that could be observed both with the naked eye and the SEM images. The surfaces of the specimens exposed to the acid attack had a white coating visible to the naked eye (Figure 3c). SEM micrographs were taken from the surface of the mortar samples (Figure 9). In the SEM images of the specimens attacked, typical gypsum acicular forms were observed (Figure 9, right). Moreover, the energy-dispersive X-ray spectroscopies (EDX) carried

out (Table 3) revealed that the mortars exposed to the acid attack contained more sulfur than the non-attacked mortars. The percentage of sulfur found in the ZS mortars attacked with the sulfuric acid solution was the lowest, while for the rest of the mortars was similar. Calcium sulfate (gypsum) is formed in a reaction of the acid with calcium hydroxide and the C-S-H phase. The chemical reactions result in a profound degradation of the hydrated cement paste, and is associated with a loss of strength (Figure 4) [38]. All carbonate-based rocks, such as limestone (used in this research), dolomite, magnesite, etc., are vulnerable to this type of attack. The results are consistent with previous experiments conducted on adobe samples and rendering mortars attacked by sulfuric acid, where the formation of gypsum patina is due to the following chemical reaction [32,44,53]:



Table 3. Energy-dispersive X-ray spectroscopy (EDX) of the mortars.

Element	Control	Control Attacked	ES	ES Attacked	ZS	ZS Attacked	NS	NS Attacked
	wt. %	wt. %	wt. %	wt. %	wt. %	wt. %	wt. %	wt. %
C	12.4	13.8	12.3	9.9	18.9	6.8	9.9	10.5
O	49.1	53.1	51.5	49.2	49.2	55.5	49.9	46.3
F	-	-	0.2	-	-	-	-	-
Mg	-	-	-	-	-	-	0.3	-
Al	1.3	-	1.1	-	0.2	-	1.1	-
Si	3.56	2.0	3.3	2.7	0.9	0.5	3.6	5.0
S	1.1	16.9	0.4	16.4	-	13.9	0.7	17.7
Ca	31.5	20.2	30.2	21.8	30.7	23.2	33.4	20.6
Fe	1.1	-	1.0	-	0.1	-	1.1	-

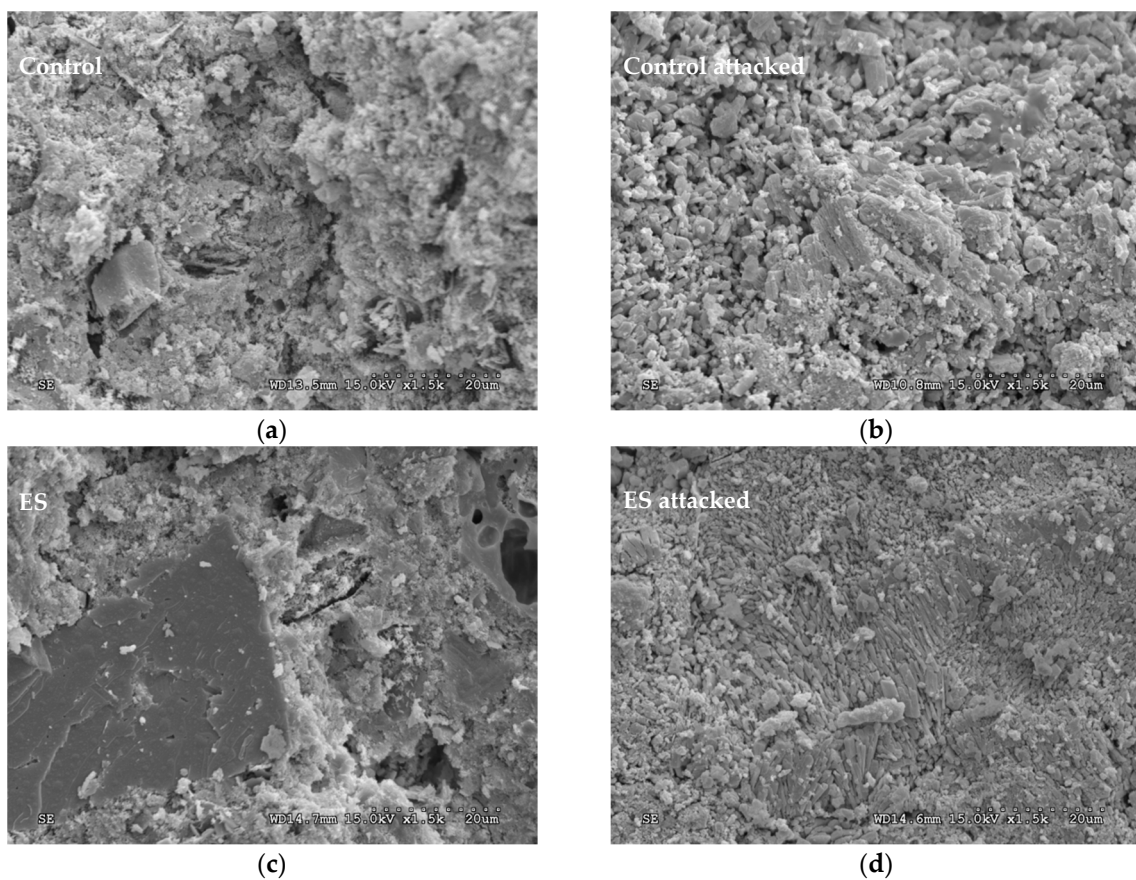


Figure 9. Cont.

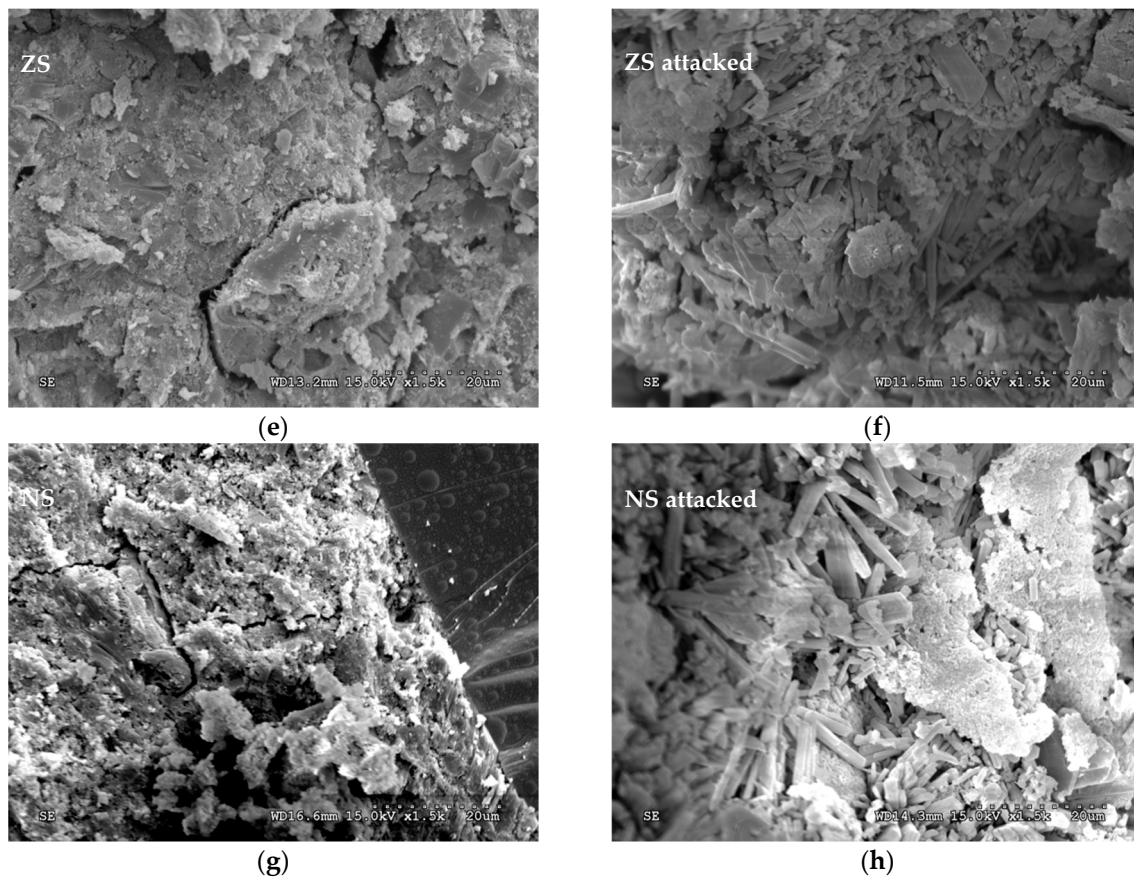


Figure 9. SEM images. Left: references mortars. (a) control mortar, (c) mortar with an ethyl silicate coating, (e) zinc stearate mortar, and (g) nanosilica mortar. Right: mortars after the sulfuric acid attack. (b) control mortar attacked, (d) mortar with an ethyl silicate coating attacked, (f) zinc stearate mortar attacked, and (h) nanosilica mortar attacked.

4. Conclusions

This work analyzed the effects of a sulfuric acid attack on the physical and mechanical properties of four different mortars: control mortar, nanosilica mortar, zinc stearate mortar, and a mortar with an ethyl silicate coating. Sulfuric acid attack has significant consequences on the microstructure and the physical and mechanical properties of the mortars. A marked loss in the mechanical properties was accompanied by microstructural alterations. In general, none of the treatments showed an obvious benefit when compared to the control sample. From the results presented in this study, the following conclusions can be drawn:

- The compressive strength of the four mortars studied decreased when they were exposed to a sulfuric acid attack. The effect on the strength reduction of the mortars was greater with longer periods of acid exposure. The control mortar had the highest compressive strength after the acid attack. However, the zinc stearate mortar had the lowest percentage of compressive strength loss after 90 days of sulfuric acid attack.
- All the mortars reduced their mass after the sulfuric acid exposure. The lowest mass loss of zinc stearate mortar proves that this mortar best resisted the acid attack.
- The zinc stearate mortar demonstrated its hydrophobic effect with the lowest coefficient of capillary water absorption, both in a non-aggressive and aggressive environment.
- Nanosilica mortar and the mortar with an ethyl silicate coating do not present positive effects when they are exposed to sulfuric acid.

- As a consequence of the sulfuric acid attack, an increase in the open porosity of mortars makes them more vulnerable to aggressive environments. Moreover, a decrease in the ultrasonic pulse velocity is detected after the acid attack.
- The results support that an alternative and reliable method of obtaining the capillary water absorption coefficient for mortars is by calculating the slope of the linear regression lines for the water absorption data as a function of time.

Author Contributions: All the authors contributed to design the research. V.E.G.-V. and A.J.T.-A. wrote the paper and performed the experiments. M.L. and J.M.S. supervised the research work and revised the paper.

Funding: This research was funded by the University of Alicante (GRE13-03) and (VIGROB-256).

Acknowledgments: The authors would like to thank Javier Pastor Moya for his technical support.

Conflicts of Interest: The authors declare no conflict of interest.

References

1. Ortega, J.M.; Esteban, M.D.; Williams, M.; Sánchez, I.; Climent, M.A. Short-term performance of sustainable silica fume mortars exposed to sulfate attack. *Sustainability* **2018**, *10*, 2517. [[CrossRef](#)]
2. Ortega Álvarez, J.; Esteban Pérez, M.; Rodríguez Escribano, R.; Pastor Navarro, J.; Sánchez Martín, I. Microstructural Effects of Sulphate Attack in Sustainable Grouts for Micropiles. *Materials* **2016**, *9*, 905. [[CrossRef](#)] [[PubMed](#)]
3. Ponikiewski, T.; Golaszewski, J. The effect of high-calcium fly ash on selected properties of self-compacting concrete. *Arch. Civ. Mech. Eng.* **2014**, *14*, 455–465. [[CrossRef](#)]
4. Glinicki, M.A.; Jozwiak-Niedzwiedzka, D.; Gibas, K.; Dabrowski, M. Influence of Blended Cements with Calcareous Fly Ash on Chloride Ion Migration and Carbonation Resistance of Concrete for Durable Structures. *Materials* **2016**, *9*, 15. [[CrossRef](#)] [[PubMed](#)]
5. Estokova, A.; Kovalcikova, M.; Luptakova, A.; Prascakova, M. Testing Silica Fume-Based Concrete Composites under Chemical and Microbiological Sulfate Attacks. *Materials* **2016**, *9*, 15. [[CrossRef](#)] [[PubMed](#)]
6. Rehman, A.U.; Qudoos, A.; Kim, H.G.; Ryou, J.-S. Influence of titanium dioxide nanoparticles on the sulfate attack upon ordinary Portland cement and slag-blended mortars. *Materials* **2018**, *11*, 356. [[CrossRef](#)] [[PubMed](#)]
7. Yu, C.; Sun, W.; Scrivener, K. Mechanism of expansion of mortars immersed in sodium sulfate solutions. *Cement Concr. Res.* **2013**, *43*, 105–111. [[CrossRef](#)]
8. Monteiro, P.J.; Kurtis, K.E. Time to failure for concrete exposed to severe sulfate attack. *Cement Concr. Res.* **2003**, *33*, 987–993. [[CrossRef](#)]
9. Wang, Z.H.; Zhu, Z.M.; Sun, X.; Wang, X.M. Deterioration of fracture toughness of concrete under acid rain environment. *Eng. Fail. Anal.* **2017**, *77*, 76–84. [[CrossRef](#)]
10. Whittaker, M.; Black, L. Current knowledge of external sulfate attack. *Adv. Cement Res.* **2015**, *27*, 532–545. [[CrossRef](#)]
11. Skalny, J.; Marchand, J.; Odler, I. *Sulfate Attack on Concrete*; Spon Press: London, UK; New York, NY, USA, 2002; ISBN 0-419-24550-2.
12. Hadigheh, S.A.; Gravina, R.J.; Smith, S.T. Effect of acid attack on FRP-to-concrete bonded interfaces. *Constr. Build. Mater.* **2017**, *152*, 285–303. [[CrossRef](#)]
13. Li, L.G.; Zhu, J.; Huang, Z.H.; Kwan, A.K.H.; Li, L.J. Combined effects of micro-silica and nano-silica on durability of mortar. *Constr. Build. Mater.* **2017**, *157*, 337–347. [[CrossRef](#)]
14. CEN EN 206-1-2013+A1:2018. *Concrete—Part 1: Specification, Performance, Production and Conformity*; AENOR: Madrid, Spain, 2018.
15. EHE-08—Code on Structural Concrete. *Articles and Annexes*; Ministerio de Fomento, Gobierno de España: Madrid, Spain, 2008; Available online: <https://www.fomento.gob.es/organos-colegiados/mas-organos-colegiados/comision-permanente-del-hormigon/cph/instrucciones/ehe-08-version-en-ingles> (accessed on 16 October 2018).
16. Ortega, J.M.; Sánchez, I.; Climent, M.A. Durability related transport properties of OPC and slag cement mortars hardened under different environmental conditions. *Constr. Build. Mater.* **2012**, *27*, 176–183. [[CrossRef](#)]

17. Norhasri, M.S.M.; Hamidah, M.S.; Fadzil, A.M. Applications of using nano material in concrete: A review. *Constr. Build. Mater.* **2017**, *133*, 91–97. [[CrossRef](#)]
18. Zhao, S.; Sun, W. Nano-mechanical behavior of a green ultra-high performance concrete. *Constr. Build. Mater.* **2014**, *63*, 150–160. [[CrossRef](#)]
19. Nik, A.S.; Bahari, A. Nano-Particles in Concrete and Cement Mixtures. *Appl. Mech. Mater.* **2011**, *110–116*, 3853–3855. [[CrossRef](#)]
20. Aitcin, P.-C. Cements of yesterday and today. *Cement Concr. Res.* **2000**, *30*, 1349–1359. [[CrossRef](#)]
21. Yu, R.; Spiesz, P.; Brouwers, H.J.H. Effect of nano-silica on the hydration and microstructure development of Ultra-High Performance Concrete (UHPC) with a low binder amount. *Constr. Build. Mater.* **2014**, *65*, 140–150. [[CrossRef](#)]
22. Adak, D.; Sarkar, M.; Mandal, S. Effect of nano-silica on strength and durability of fly ash based geopolymer mortar. *Constr. Build. Mater.* **2014**, *70*, 453–459. [[CrossRef](#)]
23. Massa, M.A.; Covarrubias, C.; Bittner, M.; Fuentesvilla, I.A.; Capetillo, P.; Von Marttens, A.; Carvajal, J.C. Synthesis of new antibacterial composite coating for titanium based on highly ordered nanoporous silica and silver nanoparticles. *Mater. Sci. Eng. C* **2014**, *45*, 146–153. [[CrossRef](#)] [[PubMed](#)]
24. Morsy, M.S.; Alsayed, S.H.; Aqel, M. Hybrid effect of carbon nanotube and nano-clay on physico-mechanical properties of cement mortar. *Constr. Build. Mater.* **2011**, *25*, 145–149. [[CrossRef](#)]
25. Navarro-Blasco, I.; Pérez-Nicolás, M.; Fernández, J.M.; Duran, A.; Sirera, R.; Alvarez, J.I. Assessment of the interaction of polycarboxylate superplasticizers in hydrated lime pastes modified with nanosilica or metakaolin as pozzolanic reactives. *Constr. Build. Mater.* **2014**, *73*, 1–12. [[CrossRef](#)]
26. Deb, P.S.; Sarker, P.K.; Barbhuiya, S. Sorptivity and acid resistance of ambient-cured geopolymer mortars containing nano-silica. *Cement Concr. Compos.* **2016**, *72*, 235–245. [[CrossRef](#)]
27. Falchi, L.; Varin, C.; Toscano, G.; Zendri, E. Statistical analysis of the physical properties and durability of water-repellent mortars made with limestone cement, natural hydraulic lime and pozzolana-lime. *Constr. Build. Mater.* **2015**, *78*, 260–270. [[CrossRef](#)]
28. Lanzón, M.; García-Ruiz, P.A. Evaluation of capillary water absorption in rendering mortars made with powdered waterproofing additives. *Constr. Build. Mater.* **2009**, *23*, 3287–3291. [[CrossRef](#)]
29. Li, W.; Wittmann, F.; Jiang, R.; Zhao, T.; Wolfseher, R. Metal Soaps for the Production of Integral Water Repellent Concrete. In *Hydrophobe VI: Water Repellent Treatment of Building Materials*; Borrelli, E., Fassina, V., Eds.; Aedificatio Publishers: Rome, Italy, 2011; pp. 145–154.
30. Soroushian, P.; Chowdhury, H.; Ghebrab, T. Evaluation of Water-Repelling Additives for Use in Concrete-Based Sanitary Sewer Infrastructure. *J. Infrastruct. Syst.* **2009**, *15*, 106–110. [[CrossRef](#)]
31. Falchi, L.; Zendri, E.; Muller, U.; Fontana, P. The influence of water-repellent admixtures on the behaviour and the effectiveness of Portland limestone cement mortars. *Cement Concr. Compos.* **2015**, *59*, 107–118. [[CrossRef](#)]
32. Lanzón, M.; Martínez, E.; Mestre, M.; Madrid, J.A. Use of zinc stearate to produce highly-hydrophobic adobe materials with extended durability to water and acid-rain. *Constr. Build. Mater.* **2017**, *139*, 114–122. [[CrossRef](#)]
33. Pigino, B.; Leemann, A.; Franzoni, E.; Lura, P. Ethyl silicate for surface treatment of concrete—Part II: Characteristics and performance. *Cement Concr. Compos.* **2012**, *34*, 313–321. [[CrossRef](#)]
34. CEN EN 933-1:2012. *Tests for Geometrical Properties of Aggregates—Part 1: Determination of Particle Size Distribution—Sieving Method*; AENOR: Madrid, Spain, 2012.
35. CEN EN 196-1:2005. *Methods of Testing Cement—Part 1: Determination of Strength*; AENOR: Madrid, Spain, 2005.
36. CEN EN 197-1:2011. *Cement—Part 1: Composition, Specifications and Conformity Criteria for Common Cements*; AENOR: Madrid, Spain, 2011.
37. CEN EN 1936:2007. *Natural Stone Test Methods—Determination of Real Density and Apparent Density, and of Total and Open Porosity*; AENOR: Madrid, Spain, 2007.
38. CEN EN 12504-4:2006. *Testing Concrete—Part 4: Determination of Ultrasonic Pulse Velocity*; AENOR: Madrid, Spain, 2006.
39. CEN EN-1015-18:2003. *Methods of Test for Mortar for Masonry—Part 18: Determination of Water Absorption Coefficient Due to Capillary Action of Hardened Mortar*; AENOR: Madrid, Spain, 2003.
40. Tixier, R.; Mobasher, B. Modeling of Damage in Cement-Based Materials Subjected to External Sulfate Attack. I: Formulation. *J. Mater. Civ. Eng.* **2003**, *15*, 305–313. [[CrossRef](#)]

41. Huang, Q.; Wang, C.; Yang, C.; Zhou, L.; Yin, J. Accelerated sulfate attack on mortars using electrical pulse. *Constr. Build. Mater.* **2015**, *95*, 875–881. [[CrossRef](#)]
42. Ma, H.; Li, Z. Microstructures and mechanical properties of polymer modified mortars under distinct mechanisms. *Constr. Build. Mater.* **2013**, *47*, 579–587. [[CrossRef](#)]
43. Bonakdar, A.; Mobasher, B. Multi-parameter study of external sulfate attack in blended cement materials. *Constr. Build. Mater.* **2010**, *24*, 61–70. [[CrossRef](#)]
44. Lanzon, M.; Garcia-Ruiz, P.A. Deterioration and damage evaluation of rendering mortars exposed to sulphuric acid. *Mater. Struct.* **2010**, *43*, 417–427. [[CrossRef](#)]
45. Komlosš, K.; Popovics, S.; Nürnbergerová, T.; Babál, B.; Popovics, J.S. Ultrasonic pulse velocity test of concrete properties as specified in various standards. *Cement Concr. Compos.* **1996**, *18*, 357–364. [[CrossRef](#)]
46. Zhou, Y.; Li, M.; Sui, L.; Xing, F. Effect of sulfate attack on the stress–strain relationship of FRP-confined concrete. *Constr. Build. Mater.* **2016**, *110*, 235–250. [[CrossRef](#)]
47. Atahan, H.N.; Arslan, K.M. Improved durability of cement mortars exposed to external sulfate attack: The role of nano & micro additives. *Sustain. Cities Soc.* **2016**, *22*, 40–48. [[CrossRef](#)]
48. Yaman, I.; Inci, G.; Yesiller, N.; Aktan, H. Ultrasonic pulse velocity in concrete using direct and indirect transmission. *ACI Mater. J.* **2001**, *98*, 450–457.
49. Toutanji, H. Ultrasonic wave velocity signal interpretation of simulated concrete bridge decks. *Mater. Struct.* **2000**, *33*, 207–215. [[CrossRef](#)]
50. Genovés, V.; Vargas, F.; Gosálbez, J.; Carrión, A.; Borrachero, M.V.; Payá, J. Ultrasonic and impact spectroscopy monitoring on internal sulphate attack of cement-based materials. *Mater. Des.* **2017**, *125*, 46–54. [[CrossRef](#)]
51. Neville, A. The confused world of sulfate attack on concrete. *Cement Concr. Res.* **2004**, *34*, 1275–1296. [[CrossRef](#)]
52. Hall, C.; Hoff, W.D. *Water Transport in Brick, Stone, and Concrete*; Spon Press: London, UK, 2002.
53. García-Vera, V.E.; Lanzón, M. Physical-chemical study, characterisation and use of image analysis to assess the durability of earthen plasters exposed to rain water and acid rain. *Constr. Build. Mater.* **2018**, *187*, 708–717. [[CrossRef](#)]



© 2018 by the authors. Licensee MDPI, Basel, Switzerland. This article is an open access article distributed under the terms and conditions of the Creative Commons Attribution (CC BY) license (<http://creativecommons.org/licenses/by/4.0/>).